

# Detection and Identification of Organic Gas Based on Intelligent Chemical Cataluminescence Array Sensors Device

Zhouxiang Shou, Yan Sun, Yuhuai Wang

Hangzhou Normal University, Qianjiang College, Hangzhou 310018, China  
 173487503@qq.com

The chemical cataluminescence sensor did not require an external light source and a complicated circuit, which avoids scattering of light, it has high sensitivity and selectivity, and has a wide linear range, so researchers have shown a great interest in this type of sensor. However, when the chemical cataluminescence sensor was used for routine analysis, it was found that there are still some deficiencies, mainly the short sensor life and signal drift caused by the consumption of luminescent reactants, thus limiting the cataluminescence sensor in practice. The application of the analysis is particularly important to develop a cataluminescence sensor with high sensitivity and stability, simple production, and long life and practical application. The continuous development of nanotechnology has provided new opportunities for the research of cataluminescence sensors. Certain gases can generate strong chemiluminescence on the surface of certain nanomaterials. Therefore, nanomaterials can be used to design different types of catalytic luminescence sensors for sensitive materials. In this paper, nano-catalysts were used as sensitive materials, and a catalyzed luminescence sensor array is designed to broaden the application range of catalytic luminescence.

## 1. Introduction

At present, the instruments for the detection of various gas samples are mainly gas chromatography, mass spectrometry, gas-mass spectrometry, etc (Li et al., 2013; Boots et al., 2014; Agapiou et al., 2015; Kluger et al., 2013; Shi et al., 2018; Khan et al., 2013). These instruments can perform comprehensive and accurate analysis of various components of gases due to the high cost and volume of these instruments, huge and complicated operations limit their wide application in production and life (Shi et al., 2012). In the actual production process, it is not possible to monitor all the components of the gas at the same time. Instead, it is only necessary to monitor the concentration of one of the components in real time, for example, to prevent gas poisoning and carbon monoxide in daily life. The measurement has received much attention from people; in order to maintain normal traffic order and the safety of people's lives, the police detect the gas exhaled by drunk drivers and measure the amount of ethanol in their exhaled breath. In order to meet people's requirements, this requires the gas sensor must have a high sensitivity, selectivity, stability, long life and small detection device features (Shi et al., 2018).

Research on cataluminescence gas sensors by using nanomaterials is a very important aspect of nanoscience research (Jin et al., 1998). It is mainly reflect in the following two aspects. Firstly, with the development of science and technology and the gradual expansion of industrial production scale, the types and quantities of gaseous materials used and gases produced in the production process are constantly increasing. These gases have certain pollution to the environment. Therefore, real-time monitoring of their concentrations is of great significance to the sustainable development of the national economy. Secondly, people's attention to their own health and their growing concern about the ecological environment have made higher demands on the monitoring and control of toxic and harmful gases in the environment (Deng et al., 2016).

Cataluminescence sensors consume only oxygen and sample molecules in the air during the luminescence process, and the fixed solid catalyst does not consume, so the nanomaterials as sensitive gas sensors overcome the disadvantages of traditional chemiluminescence sensor reagent consumption and shedding. It

is expected to develop into a new class of chemiluminescent gas sensors with practical value. It is possible to detect a substance that was originally difficult to detect due to low luminescence intensity, and it is possible to utilize a catalyst material that was originally unable to be used for analysis purposes due to its low activity. The diagram of cataluminescence sensor principle was shown in Figure 1.

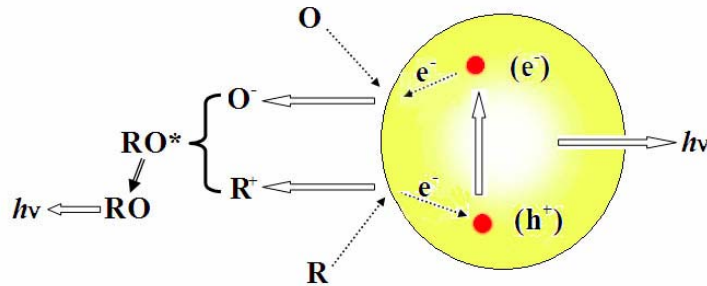


Figure 1: The diagram of cataluminescence sensor principle

## 2. The related algorithms and hardware

### 2.1 Gas sensor array

Since the signal obtained by the sensor may have noise and other interference factors, it is necessary to perform appropriate processing on the sensor signal to obtain the required data. There are many ways to deal with it, including removing redundancy, reducing noise and other operations, the so-called feature extraction. When feature extraction is performed, a series of operations are required. The methods used are relative method, difference method, logarithm method, and normalization method. Experiments showed that relative and partial differential models help to compensate for sensor gas sensitivity, and partial differential mode linearizes the relationship between sensor resistance and concentration. For example, the first derivative of the sensor signal can help distinguish between sensor drift and sample detection. The normalized effect of the sensor output is to make the input between [0,1], so each element of a single sensor response is in the same order of magnitude. The advantage is that the calculation error of the sensor itself can be reduced, and the input data of the pattern recognition can also be properly processed.

### 2.2 Classification algorithm

Principal component analysis (PCA) was used to reduce dimensionality and facilitate visualization of the sensor feature data. Based on the original variables, PCA formatted a new set of variables and termed principal components (PCs), which were linear combinations of the original variables. The first principal component (PC) captured the maximum variance, which showed the greatest variance of original data set, the second PC was orthogonal to first PC.

The data matrix  $X = \{x_{ij}\}_{I \times J}$  can be approximated by PCA as:

$$X = AB^T + E \quad (1)$$

$$A = \{a_{ir}\}_{I \times R}$$

Where A matrix contains mutually orthogonal columns with successively maximum sums of squares.

$$B = \{b_{ir}\}_{I \times R} \quad (2)$$

Where B is the columnwise orthonormal. A contains the scores of I object on R principal components. The scores are the projection of samples on principal components. The B matrix is a square matrix which contains original variables. Scores and loadings indicate the relative weights of the rows and columns for the corresponding PCs (where  $R < \min(I, J)$ ).

$$E = \{e_{ir}\}_{I \times R} \quad (3)$$

Where E matrix is the information of X which cannot be explained by the PCs. The PCA model can be alternatively written for arbitrary entry  $x_{ij}$ :

$$x_{ij} = \sum_{r=1}^R a_{ij} b_{ij} + e_{ij} \quad (4)$$

However, PCA is a linear transformation analysis method, which can only extract the linear features of data. So it is only suitable for solving linear problems. The relationship between measured gas concentration and sensor device is usually non-linear. The non-linear characteristics of experiment data can not get by PCA method.

Kernel principal component analysis (KPCA) is a signal separate method for nonlinear model based on principal component analysis. The basic idea convert the input space to feature space by nonlinear mapping, then map the data by linear PCA, which has a strong non-linear processing capability. Kernel function  $K(x, y)$ , which meet Mercer condition can achieve feature space inner operation, without the need to know specific mapping function  $\Phi$ . Let  $M$  vectors  $(x_1, x_2, x_3, \dots, x_M)$  of input space  $R$  mapping to  $\Phi(x)$  by nonlinear feature space  $F$ :

$$\Phi : \vec{R}^F, \vec{x} \cdot (x) \quad (5)$$

The mapping data covariance matrix:

$$C_F = \frac{1}{M} \sum_{j=1}^M (\Phi(x_j) - m_0^\Phi) (\Phi(x_j) - m_0^\Phi)^T \quad (6)$$

In it:

$$m_0^\Phi = \frac{1}{M} \sum_{j=1}^M \Phi(x_j) \quad (7)$$

Then:

$$\lambda (\Phi(x_j) \cdot v) = \Phi(x_j) \cdot C_F v \quad (8)$$

Characterized vector  $u$  of CF can belinear represented by  $\Phi(x_j)$ :

$$v = \sum_{j=1}^M a_j \Phi(x_j) \quad (9)$$

From formula (4) and (5):

$$\begin{aligned} & \lambda \sum_{j=1}^M a_j (\Phi(x_k) \cdot \Phi(x_j)) \\ &= \frac{1}{M} \sum_{j=1}^M a_j \left( \Phi(x_j) \cdot \sum_{i=1}^M \Phi(x_i) \right) (\Phi(x_j) \cdot \Phi(x_i)) \end{aligned} \quad (10)$$

$$k = 1, 2, \dots, M$$

Define  $M * M$  matrix  $K$ :

$$K_{ij} = \Phi(x_i) \cdot \Phi(x_j) \quad (11)$$

$$M \lambda a = K a$$

Feature vector  $u_k$  can be obtained from the feature vector  $a$  of matrix  $K$ , which is the main element orientation of mapping space:

$$v_k = \sum_{i=1}^M a_i^k \Phi(x_j) \quad (12)$$

Where  $k = 1, 2, \dots, p$ ,  $p$  is the master metadata of selected kernel function.  $v_k$  is the feature vector of enter space in test samples during F eigenvectors,  $y_k$  is projection on  $k = 1, 2, \dots, p$ :

$$y_k = v_k \cdot \Phi(x) \sum_{i=1}^M a_i^k (\Phi(x_j) \cdot \Phi(x)) \quad (13)$$

The inner product can be achieved by kernel function, namely:

$$\Phi(x_j) \cdot \Phi(x) = K(x_j, x) \quad (14)$$

### 2.3 System hardware and architecture

The cataluminescence sensor device was shown in Figure 2. The nanomaterials were first uniformly coated on a ceramic heater core and then placed in a 12mm diameter quartz tube. The temperature of the surface of the heating rod and the nanomaterial was controlled by adjusting the voltage of the heating rod, and the surface temperature thereof is measured by a thermocouple. By using pure air as the carrier gas, the flow rate of air is controlled by an adjustable gas flowmeter. When the sample gas passes through the quartz tube, it contacts with the catalyst coated on the surface of the ceramic rod and catalyzes the oxidation reaction. The photons emitted during the reaction were weak by BPCL.

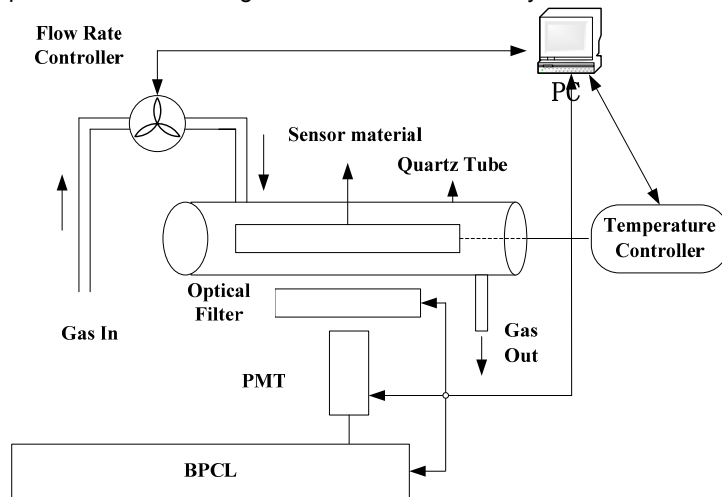


Figure 2: The cataluminescence sensor device

## 3. Experiment and results

### 3.1 Pattern recognition comparison

There were many common kernel functions used for pattern recognition, the Gaussian kernel function as following:

$$K(x, y) = \exp(-\|x - y\|^2 / c), c = 120 \quad (15)$$

Table 1: Comparison of PCA and KPCA

PCA			KPCA		
$\lambda$ value	Contribution	Cumulative contribution	$\lambda$ value	Contribution	Cumulative contribution
$\lambda_1=5.5207$	44.85%	44.85%	$\lambda_1=0.5797$	59.75%	69.75%
$\lambda_1=4.0469$	32.35%	72.21%	$\lambda_1=0.3149$	32.45%	83.73%
$\lambda_1=1.5743$	12.36%	80.14%	$\lambda_1=0.0633$	6.53%	89.73%
$\lambda_1=0.4252$	3.48%	83.62%	$\lambda_1=0.0065$	0.67%	96.37%
$\lambda_1=0.4571$	2.11%	85.73%	$\lambda_1=0.0029$	0.30%	96.40%
$\lambda_1=0.2563$	1.28%	90.14%	$\lambda_1=0.0018$	0.19%	97.14%

and PCA method was used for dimensionality reduction of raw data. Cumulative contribution rate of each main components were shown in Table 1. Both methods selected six main elements, the direct use of PCA dimension reduction method was not ideal and the contribution rate of first principal component was lower. For nonlinear problems, KPCA used for dimension reduction was better than PCA, only two cumulative contribution rates could reach 87% by KPCA.

### 3.2 Gas sensor array response

Different concentrations of acetone gas were introduced into the reaction chamber with a carrier gas flow rate of 180 mL/min. The measurement temperature was 190°C, the measurement wavelength was 460 nm, and the catalytic light emission response curve was drawn. As can be seen from Figure 3, the luminescence intensity is also increasing with the increase of acetone concentration. The shape of the three curves obtained is similar, and the maximum peak appears after injecting acetone for 4s, indicating that acetone responds quickly to this sensor.

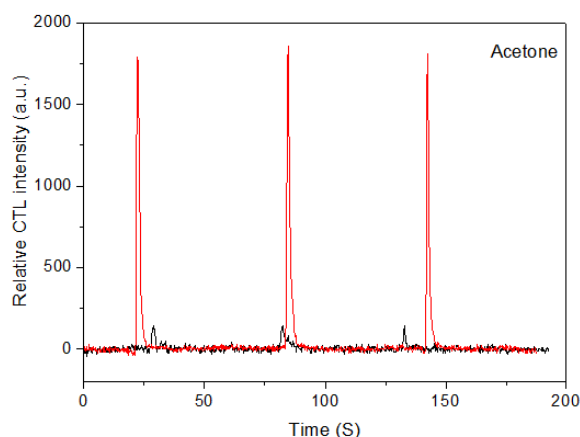


Figure 3: The catalytic light emission response curve of acetone

### 3.3 Selectivity

Under optimal conditions (temperature 190°C, wavelength 460nm, flow rate 180 mL/min), when a certain concentration of foreign substances such as acetonitrile, ammonia, n-hexane, etc. passes through this sensor, the luminescence response generated by these substances is detected. Acetone has a strong luminescence signal under this system. Acetonitrile, ammonia, n-hexane, acetone classification result was shown in Figure 4.

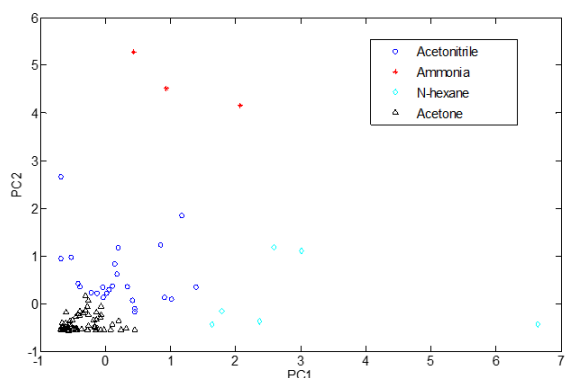


Figure 4: The classification result of acetonitrile, ammonia, n-hexane and acetone

## 4. Conclusions

Gas sensors played an important role in the detection of toxic and harmful gases, the monitoring of air pollution, and the detection of home environmental quality. With the continuous improvement of people's living

standards and the gradual emphasis on environmental protection, the requirements for sensors are also increasing. With the development of film technology and MEMS technology, gas sensors can also be better arrayed, integrated, and miniaturized. Sensing technology is a cross discipline in the field of skid science, electronic technology, and computer technology. Fingerprints output from the sensor array and pattern recognition algorithms are used to detect different gas components, which lays a solid foundation for practical gas detectors.

### Acknowledgments

This work was supported by Project of Zhejiang Public Welfare Technology Application Research Project (2017C33219), Zhejiang Provincial Department of Education General Scientific Research Project Establishment (Y201533638).

### References

- Agapiou A., Amann A., Mochalski P., Statheropoulos M., Thomas C.L.P., 2015, Trace detection of endogenous human volatile organic compounds for search, Rescue and emergency applications, *Trends in Analytical Chemistry*, 66, 158-175.
- Boots A. W., Smolinska A., van Berkel J. J., Fijten R. R., Stobberingh E. E., Boumans M. L., 2014, Identification of microorganisms based on headspace analysis of volatile organic compounds by gas chromatography-mass spectrometry, *Journal of Breath Research*, 8(2), 027106.
- Deng F., He Y., Shi G., 2016, Low-temperature cataluminescence sensor for sulfur hexafluoride utilizing coral like Zn-doped SnO<sub>2</sub> composite, *Sensors & Actuators B Chemical*, 237, 120-126.
- Hu P., 2018, Study on High Precision Mems Inertial Sensor with Increased Detection Capacitance Driven by Electromagnetism, *Chemical Engineering Transactions*, 66, 1273-1278, DOI: 10.3303/CET1866213
- Jin Z.M.D., Zhao G., Xiong S., 1988, An experimental transmission of woodchuck hepatitis virus to young chinese marmots. *Hepatology*, 8(2), 371.
- Khan M.F., Schmid S., Larsen P.E., Davis Z.J., Yan W., Stenby E.H., Boisen A., 2013, Online measurement of mass density and viscosity of pL fluid samples with suspended microchannel resonator, *Sens, Actuators B: Chem.*, 185, 456-461.
- Kluger B., Zeilinger S., Wiesenberger G., Schöfbeck D., Schuhmacher R., 2013, Detection and Identification of Fungal Microbial Volatile Organic Compounds by HS-SPME-GC-MS, *Laboratory Protocols in Fungal Biology*, Springer New York.
- Li B., Liu J., Shi G., 2013, A research on detection and identification of volatile organic compounds utilizing cataluminescence-based sensor array, *Sensors & Actuators B Chemical*, 177(177), 1167-1172.
- Shi G., He Y., Li B., 2018, Construction and analysis of multi-path propagation model for indoor short range Ultra-wideband signal based on time domain ray tracing method, *Cluster Computing*, 2018, 1-18.
- Shi G., He Y., Luo Q., 2018, Portable device for acetone detection based on cataluminescence sensor utilizing wireless communication technique, *Sensors & Actuators B Chemical*, 257, 451-459.
- Shi G., Sun B., Jin Z., 2012, Synthesis of SiO<sub>2</sub>/Fe<sub>3</sub>O<sub>4</sub> nanomaterial and its application as cataluminescence gas sensor material for ether, *Sensors & Actuators B Chemical*, 171-172(9), 699-704.